Available online at www.sciencedirect.com

ScienceDirect

Procedia Computer Science 171 (2020) 1961–1969

Procedia Computer Science

www.elsevier.com/locate/procedia

Third International Conference on Computing and Network Communications (CoCoNet'19)

Chest X-Ray Image Denoising Using Nesterov Optimization Method with Total Variation Regularization

Dang N. H. Thanh[1,*], P. Kalavathi [2], Le Thi Thanh[3], V.B. Surya Prasath[4, 5, 6, 7]

[1]*Department of Information Technology, School of Business Information Technology, University of Economics Ho Chi Minh City, VN*
[2]*Department of Computer Science and Applications, The Gandhigram Rural Institute (Deemed to be University), India*
[3]*Department of Basis Sciences, Ho Chi Minh city University of Transport, Ho Chi Minh 700000 VN*
[4]*Division of Biomedical Informatics, Cincinnati Children's Hospital Medical Center, Cincinnati, OH 45229 USA*
[5]*Department of Pediatrics, University of Cincinnati, OH USA*
[6]*Department of Biomedical Informatics, College of Medicine, University of Cincinnati, OH 45267 USA*
[7]*Department of Electrical Engineering and Computer Science, University of Cincinnati, OH 45221 USA*

Abstract

We propose a chest X-Ray image denoising method based on Total variation regularization with implementation on the Nesterov optimization method. The denoising problem is formulated in the form of the second-order cone programming problem and then it is transformed to a saddle point problem under the min-max form. The chest X-Ray images are also processed by the Anscombe transform to be appropriate for the formulated denoising problem. In the experiments, we test on chest X-Ray images of the Radiopaedia dataset. Denoising results are evaluated by using the Peak signal-to-noise ratio and the Structure similarity metrics. Based on the image quality assessment metrics, we compared images quality after denoising of the proposed method with ones of other similar denoising methods. The results confirmed that the proposed method outperforms other compared denoising methods.

Keywords: Image Denoising; Poisson Noise, Chest X-Ray Image, Medical Image, Image Restoration, Nesterov Optimization

* Corresponding author.
E-mail address: thanhdnh@ueh.edu.vn

10.1016/j.procs.2020.04.210

1. Introduction

Image denoising [1, 2, 3, 4, 5] is a common and vital problem in the field of image processing to improve digital image quality. Because digital noise usually destroys image structures, details, edges; and reduces efficiency of postprocessing tasks such as image segmentation [6, 7], image classification [8], pattern recognition [9] etc., we must remove them. Noise usually appears in digital images during being captured by digital cameras, CT/X-Ray/MRI scanners, microscopies, etc. There are some popular types of noises: Gaussian noise [10, 11, 12], Poisson noise [13, 14], impulse noise [15, 3, 16] and speckle noise [17].

In medical imaging, the Poisson noise usually appears on CT and X-Ray images. A chest X-Ray is the most popularly performed diagnostic X-Ray technique. A chest X-Ray uses a very small dose of ionizing radiation to make pictures of the inside of the chest. A chest X-Ray reproduces images of the lungs, heart, airways, blood vessels and the bones of the spine and chest [18]. Like common X-Ray images, chest X-Ray images also contain the Poisson noise. The noise influences quality of diagnosis by imaging.

To remove the Poisson noise in chest X-Ray images, there are several approaches such as filters, regularization, wavelet analysis, mathematical transformations, Principal Component Analysis (PCA), and machine learning. In this paper, we mainly focus on regularization. Regularization [19, 20, 21] is an effective approach for the image denoising problem. Rudin, Osher and Fatemi proposed an image denoising model based on the total variation regularization. The model is well-known as the ROF (**R**udin-**O**sher-**F**atemi) model [22]. However, ROF mainly focuses on the Gaussian noise, it is not very effective for the Poisson noise removal. Le el al. proposed the modified ROF model (mROF) [13] to remove the drawback of ROF. The mROF model can remove Poisson noise very well. Also based on the total variation regularization, Goldstein and Osher [23] proposed another method to remove the Gaussian noise as well as the Poisson noise. The method is implemented by the alternating direction method of multipliers (ADMM). In recent years, there are some denoising methods for the Poisson noise such as the adaptive total variation for the Poisson noise [24], the variance stabilizing transformations based method for the Poisson noise [25], the finite difference schemes with the Anscombe transform [26] and ADMM with the Anscombe transform [27].

In this paper, we propose a chest X-Ray image denoising method based on Total variation regularization with implementation on the Nesterov optimization method. The proposed method will utilize accuracy, performance of the Nesterov optimization method and effectiveness for noise removal of Total variation regularization. Our contributions focus on using the Anscombe transform [28] to convert a Poisson noisy image to a Gaussian noisy image to be suitable for processing noise by ROF that we called it to be an adaptive ROF, utilising the Nesterov optimisation method to solve the adaptive model, proposing the denoising algorithm based on the combination of the Anscombe transform and the Nesterov optimisation method. In experiments, we test the proposed method on chest X-Ray images of the Radiopaedia dataset. We utilize the peak signal-to-noise ratio (PSNR) and the structure similarity (SSIM) metrics to evaluate image quality after denoising. Otherwise, we also compare denoising results with ones of the methods such as ROF, mROF and the image denoising method of Goldstein and Osher (the Goldstein method).

The structure of the paper is organized as follows. Section II presents the image denoising problem by Total variation regularization and the proposed chest X-Ray image denoising method. Section III presents experimental results on chest X-Ray images and comparison with other similar denoising methods. Finally, Section IV concludes.

2. Proposed Image Denoising Method

2.1. Image Denoising Problem by Total Variation Regularization

Let $\left[\boldsymbol{U_{ij}}\right]_{\boldsymbol{m\times n}}, \left[\boldsymbol{V_{ij}}\right]_{\boldsymbol{m\times n}}$ be a restored grayscale image and a Gaussian noisy grayscale image, respectively, where $\boldsymbol{m}, \boldsymbol{n}$ are number of pixels by the image height and by the image width. For convenience, we consider images in a row vector by column-wise elements:

$$[u_i]_{1\times mn} = [U_{11}, \dots, U_{m1}, U_{12}, \dots, U_{m2}, \dots., U_{1n}, \dots, U_{mn}],$$
$$[v_i]_{1\times mn} = [V_{11}, \dots, V_{m1}, V_{12}, \dots, V_{m2}, \dots., V_{1n}, \dots, V_{mn}].$$

We define finite difference schemes for partial derivatives of a pixel (i, j) by columns and by rows as follows:

$$\partial_c(\cdot) = \left[\partial_c(\cdot)_{ij}\right]_{m\times n}, \qquad \partial_r(\cdot) = \left[\partial_r(\cdot)_{ij}\right]_{m\times n},$$

where $\partial_c(\cdot), \partial_r(\cdot)$ are directional gradients by columns and by rows:

$$\partial_c(\cdot)_{ij} = \frac{(\cdot)_{i,j+1} - (\cdot)_{i,j-1}}{2}, \qquad \partial_r(\cdot)_{ij} = \frac{(\cdot)_{i+1,j} - (\cdot)_{i-1,j}}{2}.$$

We denote gradient approximation for each pixel (i, j) by:

$$\left[D_{ij}(\cdot)\right]_{2\times 1} = \begin{bmatrix}\partial_c(\cdot)_{ij} \\ \partial_r(\cdot)_{ij}\end{bmatrix}.$$

Therefore, for the vector u, we have:

$$\left[D_{ij}(u)\right]_{2\times mn} = \left[D_{ij}(U_{11}), \dots, D_{ij}(U_{mn})\right].$$

We denote

$$[D(\cdot)]_{2mn\times mn} = \begin{bmatrix}D_{11}(\cdot) \\ \vdots \\ D_{mn}(\cdot)\end{bmatrix}.$$

The image denoising problem by the Total variation regularization for the Gaussian noise can be formulated as the following constrained optimization problem:

$$u = \min_u\{TV(u)\}, \qquad \text{constraints to } |u - v|_2 \le \delta, \tag{1}$$

where

$$TV(u) = \sum_{i=1}^{m}\sum_{j=1}^{n}\left|D_{ij}(u)\right|_2 - \text{Total variation}, \tag{2}$$

and $|\cdot|_2$ is a L^2 norm, $\delta > 0$.

2.2. Chest X-Ray Image Denoising Method with the Nesterov Optimization Method

Since noise on chest X-Ray images follows by the Poisson distribution, we must transform a Poisson noisy data to a Gaussian noisy data. Suppose that $\left[\Phi_{ij}\right]_{m\times n}$ is a noisy chest X-Ray image (a Poisson noisy image). The corresponding vectorized image is $[\phi_i]_{1\times mn} = [\Phi_{11}, \dots, \Phi_{m1}, \Phi_{12}, \dots, \Phi_{m2}, \dots., \Phi_{1n}, \dots, \Phi_{mn}]$.

Our goal is to utilize the Anscombe transform [28]:

$$v = 2\sqrt{\phi + \frac{3}{8}} \tag{3}$$

to convert the Poisson noisy image ϕ to a Gaussian noisy image and then we can apply the model (1) to remove the noise. The acquired restored image u by the model (1) will be converted to the final image by the inverse Anscombe transform [28]:

$$u^* = \left(\frac{u}{2}\right)^2 - \frac{3}{8}. \tag{4}$$

Let consider the dual problem of the optimization problem (1):

$$w = arg\max_w\{-\delta|D^T(w)|_2 + v^T D^T(w)\}, \text{ with constraint } \left|w_j\right|_2 \le 1, j = 1, \dots, mn, \tag{5}$$

where w is a dual variable.

To solve the model (1) by the Nesterov optimization method [29], we consider the following min-max problem associating with (1) and (5):

$$\min_{u\in\Omega_1}\max_{w\in\Omega_2} w^T D u, \tag{6}$$

where

$$\Omega_1 = \{u: |u - v|_2 \le \delta\}, \qquad \Omega_2 = \left\{w: \left|w_j\right|_2 \le 1, j = 1, \dots, mn\right\}.$$

On Ω_1 and Ω_2, we defined the following functions:

$$f_1(u) = \frac{1}{2}|u - v|_2^2, \qquad f_2(w) = \frac{1}{2}|w|_2^2.$$

Their boundary conditions are:

$$\Delta_1 = \max_{u\in\Omega_1} f_1(u) = \frac{1}{2}\delta^2, \qquad \Delta_2 = \max_{w\in\Omega_2} f_2(w) = \frac{1}{2}mn.$$

On Ω_2, we approximate $TV(u)$ by:

$$TV_\mu(u) = \max_{w\in\Omega_2}\{w^T D(u) - \mu f_2(w)\}. \quad (7)$$

Hence,

$$TV_\mu(u) \le TV(u) \le TV_\mu(u) + \mu\Delta_2.$$

We fixed $\mu = \epsilon/(2\Delta_2) = \epsilon/(mn)$. According to the result of [29], $TV_\mu(u)$ has Lipschitz continuous derivatives if the following condition is fulfilled:

$$\mathcal{L}_\mu = \frac{|D|_2^2}{\mu} \le \frac{8}{\mu}, \quad (8)$$

and its gradient:

$$\nabla TV_\mu(u) = D^T w. \quad (9)$$

Details of the proposed chest X-Ray image denoising method based on the Nesterov optimization methods is presented in Algorithm 1.

Algorithm 1. The Chest X-Ray Image Denoising Method by the Nesterov Optimization Method.

Input: The input noisy images ϕ.
Output: The restored images u^*.

Function $u^* = \boldsymbol{Denoise}(\phi)$

Initialize: $\epsilon, \delta \leftarrow 0.96\sqrt{mn}, \mu \leftarrow \epsilon/(2mn)\,, \mathcal{L}_\mu = 8/\mu\,, k \leftarrow 0.$

Transform: $v \leftarrow 2\sqrt{\phi + 3/8}.$

Set $u^{[0]} \leftarrow v$.

Repeat

- **Compute**:

$$w^{[k]} = \underset{w\in\Omega_2}{\operatorname{argmax}}\left\{w^T D u^{[k]} - \frac{\mu}{2}\left|u^{[k]}\right|_2^2\right\}.$$

$$g^{[k]} = D^T w^{[k]}.$$

$$h^{[k]} = \underset{u\in\Omega_1}{\operatorname{argmin}}\left\{\left(u - u^{[k]}\right)^T g^{[k]} + \frac{1}{2}\mathcal{L}_\mu\left|u - u^{[k]}\right|_2^2\right\}.$$

$$s^{[k]} = \underset{u\in\Omega_1}{\operatorname{argmin}}\left\{\mathcal{L}_\mu f_1(u) + \sum_{i=1}^{k}\frac{i+1}{2}\left(u - u^{[i]}\right)^T g^{[k]}\right\}.$$

$$u^{[k+1]} = \frac{k+1}{k+3}h^{[k]} + \frac{2}{k+3}s^{[k]}.$$

$$k \leftarrow k + 1.$$

Until $\left(\sum_{i=1}^{m}\sum_{j=1}^{m}\left|D_{ij}u\right|_2 + \delta|D^T w|_2 - w^T D v < \epsilon\right)$

Transform: $u^* = (u/2)^2 - 3/8$

End.

3. Experimental Results and Discussions

We implement the proposed image denoising method on MATLAB 2018b. The computing system configuration is Windows 10 pro, 4GB RAM, CPU Intel core i5.

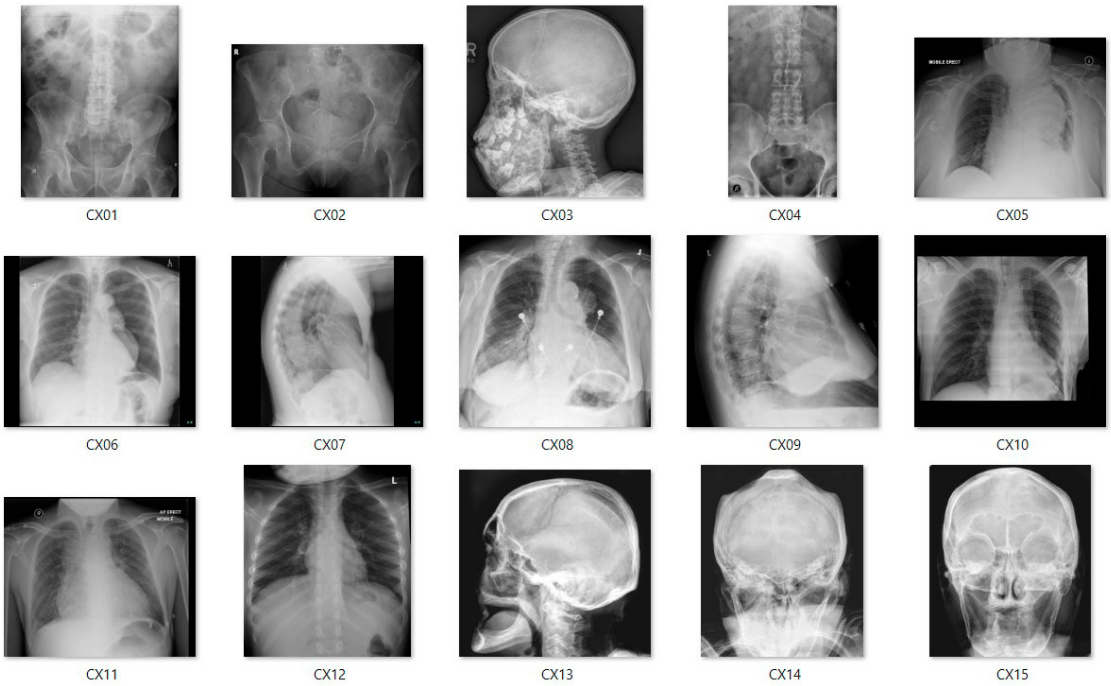

Fig. 1. Several selected chest X-Ray images.

3.1. Image Quality Assessment Metrics

To compare image quality after denoising, it is necessary to use image quality assessment metrics. In this paper, we use full reference image quality assessment metrics such as the Peak signal-to-noise ratio (PSNR) and the Structure Similarity (SSIM). They are the most common metrics [11, 5, 30].

The PSNR metric [30, 31] is defined as follows:

$$PSNR = 10\log_{10}\left(\frac{U_{max}^2}{MSE}\right) dB, \tag{10}$$

where

$$MSE = \frac{1}{mn}\sum_{i=1}^{m}\sum_{j=1}^{n}\left(U_{ij}^* - U_{ij}\right)^2 \tag{11}$$

is the mean squared error, U_{max} denotes the maximum grey value, for e.g. for an 8-bit image $U_{max} = 255$; U_{ij} and U_{ij}^* are grey values of U and U^* at each pixel (i, j), U^* is a ground truth. The higher PSNR, the better image quality.

Structural similarity (SSIM) [30, 31] is a better error metric for comparing the image quality. SSIM value is between 0 and 1 with higher value indicating better structure preservation. The SSIM metric based on the characteristic of the human vision and it is computed between two images U and U^*,

$$SSIM = \frac{(2\mu_U\mu_{U^*} + c_1)(2\sigma_{UU^*} + c_2)}{(\mu_U^2 + \mu_{U^*}^2 + c_1)(\sigma_U^2 + \sigma_{U^*}^2 + c_2)}, \tag{12}$$

where μ_U, μ_{U^*} – the average value of U, U^*; $\sigma_U^2, \sigma_{U^*}^2$ – the variance of U, U^*; σ_{UU^*} – the covariance, and c_1, c_2 are numerical stabilizing parameters, $c_1 = (K_1L)^2, c_2 = (K_2L)^2, K_1 = 0.01, K_2 = 0.03$; and $L = 255$ for an 8-bit image.

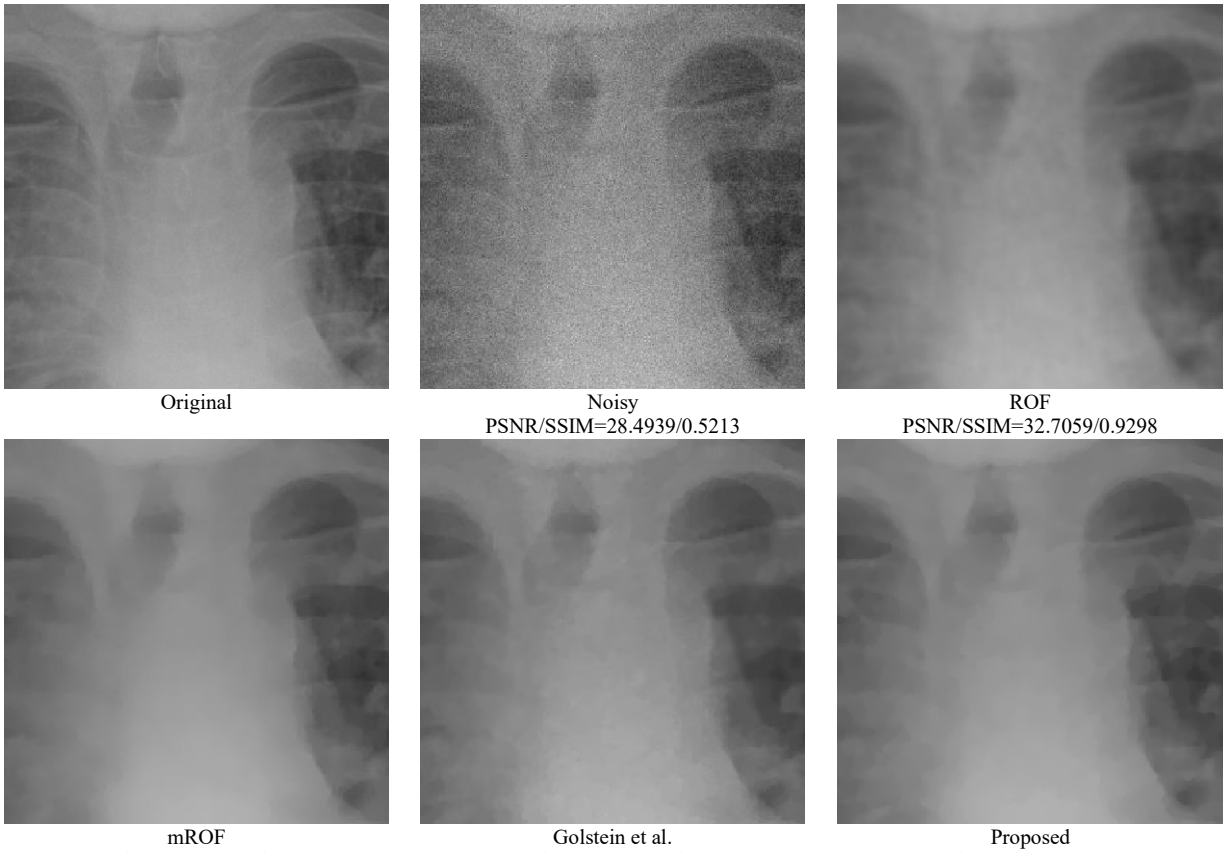

Fig. 2. Denoising results by the methods for the chest X-Ray image CX11 (300x300).

3.2. Chest X-Ray Images Dataset

We test the proposed denoising methods on chest X-Ray images of the Radiopaedia dataset†. All images are in DICOM format. They are grayscale; and width/height size varies from 579 up to 1024 pixels. We extract some frames and save as the JPEG format. We select 15 images as in Figure 1.

We must notice that, all images of the dataset are processed, and we can consider them as noise-free images (ground truth). We use the built-in *imnoise* function of MATLAB to generate the Poisson noise. This method is helpful to assess image quality, because both the PSNR and SSIM metrics need a ground truth.

Since the Poisson noise is a type of signal-dependent noise, we cannot control the noise density. The *imnoise* function for the Poisson noise has no parameter to control noise density. Although there are several methods to change the Poisson noise density such as scale noise technique, we do not use in this paper.

3.3. Experimental Results and Discussion

For the first test case, we test denoising methods such as ROF, mROF, the Goldstein method and the proposed method on the CX11 image. The denoising results for the CX11 image are showed in Figure 2. As we can see, noise destroyed image structure and made bones look weaker. The denoising result by ROF is slightly blurred. mROF made sternum be solider and smoother. Goldstein method and the proposed method denoised very well. However,

† *https: // radiopaedia.org/encyclopaedia/cases/all?modality=X-ray*

structure of ribs in our result is clearer than ones of Goldstein method. The PSNR and SSIM values of denoising results by ROF, mROF, Goldstein method and the proposed method are 32.7059/0.9298, 37.0503/0.9509, 39.5093/0.9444 and **39.8149/0.9532**. We can see that, the PSNR and SSIM values of our method are the highest.

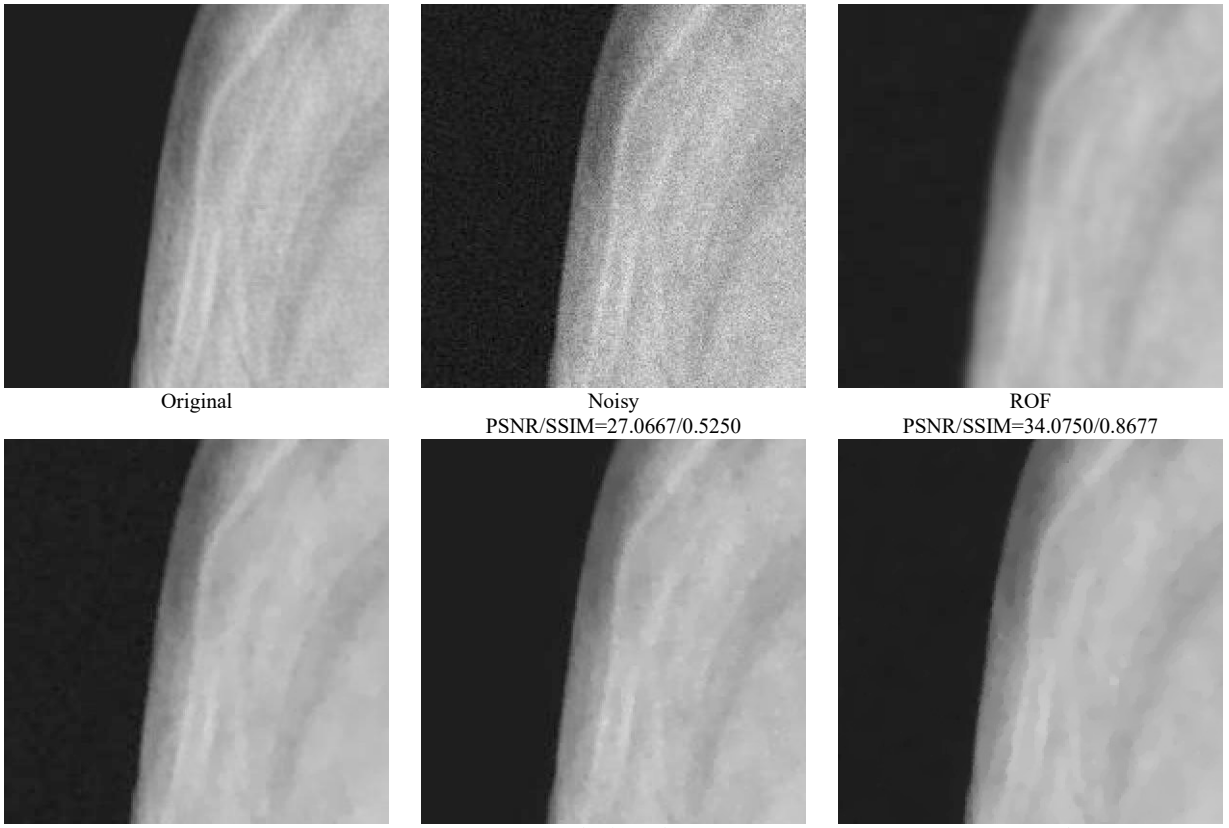

Fig. 3. Denoising results by the methods for the chest X-Ray image CX14 (200x200).

Table 1. The PSNR values of denoising results of the methods.

Name	Noisy	ROF	mROF	Goldstein et al.	Proposed
CX01	27.4338	35.7951	36.9659	36.9121	**37.2046**
CX02	29.4507	36.9332	36.9748	38.3754	**39.0537**
CX03	27.7650	34.4210	36.1265	36.6218	**36.6901**
CX04	28.2436	35.1646	38.5022	38.1345	**38.5706**
CX05	28.3433	32.9746	36.6970	38.2930	**38.5402**
CX06	27.3039	31.7394	34.2925	38.1987	**38.3099**
CX07	28.3823	33.6070	35.6633	40.0005	**40.1146**
CX08	26.6010	35.0223	36.5086	36.3487	**36.6613**
CX09	27.6649	39.3062	38.5292	39.3632	**39.4039**
CX10	29.8209	33.7173	34.1135	37.2306	**37.8964**
CX11	28.4939	32.7059	37.0503	39.5093	**39.8149**
CX12	28.7246	37.8702	38.2791	39.5432	**39.98**
CX13	27.7971	33.5548	35.0829	35.6259	**35.7701**
CX14	27.0667	34.0750	36.5140	36.1455	**36.5257**
CX15	27.4135	33.5157	36.2065	36.0026	**36.3659**
Mean	28.0337	34.6935	36.5004	37.7537	**38.0601**

For the second case, we test the methods on the CX14 image. Denoising results are presented in Figure 3. We can see that noise on the high intensity region (the bright region) is more clearly than on the low intensity region (the dark region). As in the above case, the denoising result by ROF is slightly blurred. mROF denoised well, but the

dark region contains many defects (artefacts). The Goldstein method removed noise very well, but the bone structure is sharpened much. Our method removed noise very well. There is no artefact in the dark and bright regions. The bone structure is smoothed naturally. The PSNR and SSIM values of the proposed method are the highest: ROF (34.0750/0.8677), mROF (36.5140/0.8999), Goldstein method (36.1455/0.8997) and the proposed method (**36.5257/0.9002**).

Table 1 presents PSNR values of denoising results of the considered methods. Table 2 presents SSIM values of denoising results of the methods. The proposed method gave the highest PSNR values as well as the highest SSIM values. Hence, we can affirm that the proposed method outperforms other compared method.

Table 2. The SSIM values of denoising results of the methods.

Name	Noisy	ROF	mROF	Goldstein et al.	Proposed
CX01	0.4772	0.8681	0.8856	0.8814	**0.8878**
CX02	0.5630	0.9083	0.9079	0.9144	**0.9258**
CX03	0.5503	0.8814	0.9029	0.9067	**0.9108**
CX04	0.5022	0.9295	0.9413	0.9387	**0.9421**
CX05	0.5241	0.8943	0.9075	0.9065	**0.9111**
CX06	0.5103	0.9089	0.9303	0.9207	**0.9358**
CX07	0.6061	0.9427	0.9517	0.9450	**0.9565**
CX08	0.4472	0.8686	0.8923	0.8918	**0.8929**
CX09	0.5115	0.9442	0.9453	0.9382	**0.9462**
CX10	0.7039	0.8665	0.8767	0.8983	**0.8991**
CX11	0.5213	0.9298	0.9509	0.9444	**0.9532**
CX12	0.5255	0.9325	0.9376	0.9390	**0.9445**
CX13	0.5995	0.8719	0.8922	0.9012	**0.9015**
CX14	0.5250	0.8677	0.8999	0.8997	**0.9002**
CX15	0.5699	0.8653	0.8993	0.8984	**0.8994**
Mean	0.5425	0.8986	0.9148	0.915	**0.9205**

For execution time, all above methods work very fast. They only take up 3 seconds to process a chest X-Ray image. The Goldstein method and the proposed method are faster than ROF and mROF.

4. Conclusions

In this paper, we have proposed a chest X-Ray image denoising method based on Total variation regularization with the Nesterov optimization method. The proposed method can remove noise very well, avoids creating artefacts and smooths image structures naturally. From above experimental results, it can be affirmed that the proposed method outperforms the compared denoising methods.

In future works, we would like to extend the paper to process noise of 3D volumetric medical images. This research is very important in the medical imaging. Although the proposed method can be extended to 3D images easily, optimization of processing performance requires further research.

Acknowledgement

This work was supported by Science and Engineering Research Board (SERB), Department of Science and Technology, Government of India. This research is funded by University of Economics Ho Chi Minh City, Vietnam.

References

[1] J. Shim, M. Yoon and Y. Lee, “Feasibility of newly designed fast non local means (FNLM)-based noise reduction filter for X-ray imaging: A simulation study,” *Optik,* vol. 160, pp. 124-130, 2018.

[2] R. Rojas and P. Rodriguez, “Spatially Adaptive Total Variation Image Denoising Under Salt and Pepper noise,” in *19th European Signal Processing Conference EUSIPCO*, pp 278-282, Barcelona, 2011.

[3] D. N. H. Thanh, V. B. S. Prasath and L. T. Thanh, “Total Variation L1 Fidelity Salt-and-Pepper Denoising with Adaptive Regularization Parameter,” in *IEEE 5th Nafosted Conference on Information and Computer Science NCIS'18*, Ho Chi Minh city, 2018.

[4] D. N. H. Thanh and S. Dvoenko, “A denoising of biomedical images,” *The International Archives of Photogrammetry, Remote Sensing and*

Spatial Information Sciences, vol. XL, no. 5, pp. 73-78, 2015.

[5] V. B. S. Prasath, D. N. H. Thanh and N. H. Hai, "Regularization Parameter Selection in Image Restoration with Inverse Gradient: Single Scale or Multiscale," in *IEEE 7th International Conference on Communications and Electronics*, pp. 278-282, Hue, 2018.

[6] D. N. H. Thanh, E. Uğur, V. B. S. Prasath, V. Kumar and N. N. Hien, "A Skin Lesion Segmentation Method for Dermoscopic Images Based on Adaptive Thresholding with Normalization of Color Models," in *IEEE 2019 6th International Conference on Electrical and Electronics Engineering*, Istanbul, 2019.

[7] D. N. H. Thanh, N. N. Hien, V. B. S. Prasath, L. T. Thanh and N. H. Hai, "Automatic Initial Boundary Generation Methods Based on Edge Detectors for the Level Set Function of the Chan-Vese Segmentation Model and Applications in Biomedical Image Processing," in *The 7th International Conference on Frontiers of Intelligent Computing: Theory and Application (FICTA-2018)*, Danang, 2018.

[8] A. Krizhevsky, I. Sutskever and G. E. Hinton, "ImageNet classification with deep convolutional neural networks," *Communications of the ACM ,* vol. 60, no. 6, pp. 84-90 , 2017.

[9] V. Naghashi, "Co-occurrence of adjacent sparse local ternary patterns: A feature descriptor for texture and face image retrieval," *Optik,* vol. 157, p. 877–889, 2018.

[10] D. Chen, Y. Q. Chen and D. Xue, "Fractional-order total variation image denoising based on proximity algorithm," *Applied Mathematics and Computation,* vol. 257, pp. 537-545, 2015.

[11] V. B. S. Prasath, D. N. H. Thanh and N. H. Hai, "On Selecting the Appropriate Scale in Image Selective Smoothing by Nonlinear Diffusion," in *IEEE 7th International Conference of Communications and Electronics*, pp. 267-272, Hue, 2018.

[12] D. Jinming, L. Wenqi, P. Zhenkuan and B. Li, "New second order Mumford–Shah model based on Γ-convergence approximation for image processing," *Infrared Physics & Technology,* vol. 76, pp. 641-647, 2016.

[13] T. Le, R. Chartrand and T. J. Asaki, "A Variational Approach to Reconstructing Images Corrupted by Poisson Noise," *Journal of Mathematical Imaging and Vision,* vol. 27, no. 3, pp. 257-263, 2007.

[14] D. N. H. Thanh, V. B. S. Prasath and L. M. Hieu, "A Review on CT and X-Ray Images Denoising Methods," *Informatica,* vol. 43, no. 2, pp. 151-159, 2019.

[15] T. Chen and H. R. Wu, "Adaptive impulse detection using center-weighted median filters," *IEEE Signal Processing Letters,* vol. 8, no. 1, pp. 1-3, 2001.

[16] D. N. H. Thanh, L. T. Thanh, N. N. Hien and V. B. S. Prasath, "Adaptive Total Variation L1 Regularization for Salt and Pepper Image Denoising," *Optik - International Journal for Light and Electron Optics,* 2020 (In Press).

[17] A. Saadia and A. Rashdi, "A Speckle Noise Removal Method," *Circuits, Systems, and Signal Processing,* vol. 37, no. 6, p. 2639–2650, 2018.

[18] Radiological Society of North America, [Online]. Available: https://www.radiologyinfo.org/en/info.cfm?pg=chestrad. [Accessed 25 8 2019].

[19] D. N. H. Thanh and S. Dvoenko, "Image noise removal based on Total Variation," *Computer Optics,* vol. 39, no. 4, pp. 564-571, 2015.

[20] H. Hu and J. Froment, "Nonlocal Total Variation for Image Denoising," in *IEEE 2012 Symposium on Photonics and Optoelectronics*, Shanghai, 2012.

[21] P. Jidesh and H. K. Shivarama, "Non-local total variation regularization models for image restoration," *Computers & Electrical Engineering,* vol. 67, pp. 114-133, 2018.

[22] L. Rudin, S. Osher and E. Fatemi, "Nonlinear total variation based noise removal algorithms," *Physica D,* vol. 60, no. 1-4, pp. 259-268, 1990.

[23] T. Goldstein and S. Osher, "The split Bregman method for L1-regularized problems," *SIAM Journal on Imaging Sciences,* vol. 2, no. 3, p. 323–343, 2009.

[24] V. B. S. Prasath, "Quantum Noise Removal in X-Ray Images with Adaptive Total Variation Regularization," *Informatica,* vol. 28, no. 3, pp. 505-515, 2017.

[25] M. Markku and F. Alessandro, "Optimal Inversion of the Anscombe Transformation in Low-Count Poisson Image Denoising," *IEEE Transactions on Image Processing,* vol. 20, no. 1, pp. 99-109, 2011.

[26] L. T. Thanh and D. N. H. Thanh, "Medical Images Denoising Method Based on Total Variation Regularization and Anscombe Transform," in *IEEE The 19th International Symposium on Communications and Information Technologies (ISCIT 2019)*, Ho Chi Minh city, 2019.

[27] N. H. Hai, D. N. H. Thanh, N. N. Hien, C. Premachandra and S. Prasath, "A Fast Denoising Algorithm for X-Ray Images with Variance Stabilizing Transform," in *The 11th IEEE Internation Conference on Knowledge and Systems Engineering (KSE 2019)*, Danang, 2019.

[28] F. J. Anscombe, "The transformation of Poisson, binomial and negative-binomial data," in *Biometrika*, Oxford , Oxford University Press, 1948, p. 246–254.

[29] J. Dahl, P. C. Hansen, S. H. Jensen and T. L. Jensen, "Algorithms and software for total variation image reconstruction via first-order methods," *Numer Algor,* vol. 53, pp. 67-92, 2010.

[30] Z. Wang, A. Bovik, H. Sheikh and E. Simoncelli, "Image quality assessment: From error visibility to structural similarity," *IEEE Transactions on Image Processing,* vol. 13, no. 4, pp. 600-612, 2004.

[31] V. B. S. Prasath and D. N. H. Thanh, "Structure tensor adaptive total variation for image restoration," *Turkish Journal of Electrical Engineering & Computer Sciences,* vol. 27, no. 2, pp. 1147-1156, 2019.